minerals

MDPI

Article

Magmatic Process Associated with the Baogutu Reduced Cu Porphyry-Type Deposit (West Junggar, Northwest China): Evidence from Multiple Enclaves

Chu Wu [1], Tao Hong [2,3,*], Xing-Wang Xu [4,5,6,*], Xiao Zheng [1], Cheng-Xi Wang [1], Wan-Juan Liang [1], Ke-Feng Sun [1], Hui-Jun Zhang [1], Bin Wang [1] and Lian-Hui Dong [4,7]

1 Development and Research Center of China Geology Survey, Beijing 100037, China; wuchu@mail.cgs.gov.cn (C.W.); zxiao@mail.cgs.gov.cn (X.Z.); wchengxi@mail.cgs.gov.cn (C.-X.W.); lwanjuan@mail.cgs.gov.cn (W.-J.L.); skefeng@mail.cgs.gov.cn (K.-F.S.); zhuijun@mail.cgs.gov.cn (H.-J.Z.); wangbincgs@mail.cgs.gov.cn (B.W.)
2 Guangdong Provincial Key Lab of Geodynamics and Geohazards, School of Earth Sciences and Engineering, Sun Yat-sen University, Guangzhou 510275, China
3 Southern Marine Science and Engineering Guangdong Laboratory (Zhuhai), Zhuhai 519082, China
4 Key Laboratory of Mineral Resources, Institute of Geology and Geophysics, Chinese Academy of Sciences, Beijing 100029, China; tjdlh@263.net
5 College of Earth and Planetary Sciences, University of Chinese Academy of Sciences, Beijing 100049, China
6 Institutions of Earth Science, Chinese Academy of Sciences, Beijing 100029, China
7 Xinjiang Bureau of Geology and Mineral Resources, Urumqi 830000, China
* Correspondence: hongt5@mail.sysu.edu.cn (T.H.); xuxw@mail.iggcas.ac.cn (X.-W.X.)

check for updates

Citation: Wu, C.; Hong, T.; Xu, X.-W.; Zheng, X.; Wang, C.-X.; Liang, W.-J.; Sun, K.-F.; Zhang, H.-J.; Wang, B.; Dong, L.-H. Magmatic Process Associated with the Baogutu Reduced Cu Porphyry-Type Deposit (West Junggar, Northwest China): Evidence from Multiple Enclaves. *Minerals* **2022**, *12*, 815. https://doi.org/10.3390/min12070815

Academic Editor: Massimo D'Antonio

Received: 3 May 2022
Accepted: 23 June 2022
Published: 26 June 2022

Abstract: Enclaves constitute a key tracer guide to assess the magmatic source and evolutionary processes of Cu–Mo–Au porphyry-type deposits. In this study, four types of enclaves were identified in the Baogutu reduced Cu porphyry-type deposit, West Junggar, Northwest China: gabbroic enclaves (Type 1) and schist enclaves (Type 2) are proposed to be restites and immiscible enclaves, respectively, which confirm the contributions of mantle components and sediments in the reduced Cu porphyry-type deposit. Fine-grained dioritic enclaves (Type 3) have a similar mineral composition and texture to the dioritic host rocks, which are probably autoliths derived from inhomogeneous fractional crystallization. Tuffaceous siltstone enclaves (Type 4) with a zircon U-Pb age of 339.2 ± 7.5 Ma (MSWD = 0.55), the formation age of which is in agreement with the host early Carboniferous rock unit, indicate that these tuffaceous siltstone enclaves might have formed in a contamination process. Moreover, the schist enclaves, together with the newly discovered 2691.3 ± 12.3 Ma inherited zircon in tuffaceous siltstone enclaves, further indicate that the Baogutu arc could be a continental arc.

Keywords: petrogenesis of enclaves; magmatic evolution; continental island arc; Baogutu reduced Cu porphyry-type deposit

1. Introduction

Porphyry-type mineral deposits supply the most economically important class of Cu, Mo, Au, W, and Sn mineral resources [1,2]. These are typically magmatic–hydrothermal mineralizing systems associated with intermediate-felsic porphyritic intrusions and occur in convergent margins [2–4]. It is widely accepted that porphyry-type deposits are formed by the precipitation of hydrothermal minerals from aqueous solutions. They are normally indicated by disseminated, vein-, stockwork-, and breccia-hosted mineralization with oxidized ore-forming conditions [5,6]. The Baogutu deposit is a special "reduced"-Cu porphyry-type deposit, which contains abundant hypogene pyrrhotite and methane-rich fluid inclusions, with a relatively lower Cu tonnage than classic oxidized Cu porphyry-type deposit [7]. There are two different viewpoints regarding the formation mechanism of the Baogutu reduced Cu porphyry-type deposit. On the one hand, Shen and Pan [8] suggest

the Baogutu magma was derived from the partial melting of a metasomatized mantle wedge, which underwent significant contamination after emplacement, with the reduced component originating from the country-rock. On the other hand, Cao et al. [9,10] suggest that reduced granitoids were formed through the mixing of mantle-derived mafic magma, juvenile lower crust-derived felsic magma, subducted oceanic sediments, and asthenosphere mantle. Moreover, the mantle-derived CO_2 was reduced to CH_4 via the Fischer–Tropsch reaction during the magmatic process, contributing to the reduced ore-forming conditions [11]. However, the lack of convincing petrological evidence has hampered our understanding of reduced Cu porphyry-type deposits.

Enclaves are widely preserved in porphyry-type deposits and thus present an excellent opportunity to explore the process of magmatic to hydrothermal transition, e.g., the sulfide-bearing enclaves in the Bingham Cu porphyry-type deposit, in detail. Utah suggests the heterogeneous distribution of Cu sulfides in the magma source [12]; the mafic microgranular enclaves in the Dabu Cu porphyry-type deposit, Tibet, indicate that the reaction between the mafic and felsic magmas might have further increased Cu concentrations and contributed to subsequent mineralization [13]; the microgranular enclaves in the Tulasu ore cluster, Xinjiang, produced the Cu–Au metallogenic connection between the porphyry magma and epithermal fluid [14]; and the fine-grained dioritic enclaves in the Sanchakou Cu porphyry-type deposit, Eastern Tianshan, recorded the inhomogenous differentiation of magma [15]. Importantly, many enclaves have previously been discovered in the Baogutu reduced Cu porphyry-type deposit; however, research concerning their features, varieties, and origins has not been conducted. In this study, we focused on both the newly defined and previously studied enclaves and their relationships with host rocks and mineralization in terms of the Baogutu deposit. We integrated petrographical and geochronological studies with published data concerning the enclaves and wall rocks to: (1) define the petrogenesis of enclaves; (2) determine the magmatic process in the Baogutu reduced Cu porphyry-type deposit.

2. Geological Setting

2.1. Regional Geology

The West Junggar region is located in the core of the west domain of the Central Asian Orogenic Belt (CAOB, Figure 1a) [16–18]. It encompasses six tectonic units from north to south: Sawuer oceanic island arc (OIA), Xiemisitai OIA, Barluk continental arc (CA), Barluk–Mayile–Tangbale–Darbut (BMTD) ophiolite belt, Baogutu arc, and Laba–Junggar terrane (Figure 1b) [19,20]. The Sawuer and Xiemisitai arcs, which are considered to be oceanic island arcs in the Paleo-Asian Ocean, are characterized by the occurrence of Early Paleozoic adakites, porphyry-type deposits, and calc–alkaline granites [5,18,21]. The Barluk arc contains abundant Precambrian-inherited zircons, which indicates that a Late Paleozoic continental arc might occur in the east margin of the Kazakhstan continent during the westward subduction of the Junggar Oceanic plate [19]. Ophiolites in the Mayile, Tangbale, Barluk, Darbut, and Karamay areas (BMTD ophiolite belt) are likely to represent the residue of the Junggar oceanic plate, which has been invaded by late Carboniferous granite plutons and unconformably overlay by late Carboniferous–Permian strata [18–23].

The Baogutu arc, located between the BMTD ophiolite belt and Laba–Junggar terrane, is sandwiched between the Darbut ophiolite belt and Karamay–Baijiantan ophiolite belt (Figure 1b) [16,19,20]. The Early Paleozoic (ca. 426–368 Ma) Darbut ophiolite belt represents the southeastern margin of the Junggar oceanic plate, and mainly consists of wehrlite clinopyroxene peridotite, cumulated gabbro, pyroxenite, diabase, pillow lava, and chert, and contains some metamorphic blocks [19,20,24,25]. The Baogutu arc was probably formed during the southeastward subduction of the Junggar oceanic plate, which is considered to have been an island arc [10,19,20]. The majority of the Baogutu arc comprises Carboniferous volcanic, volcaniclastic, and sedimentary rocks with three sequences: (1) the lower part is composed of basalt, andesite, diabase, tuff, plagioclase-bearing crystal tuff, volcanic breccia, interbedded by minor siliceous rocks (possibly chert), muddy siltstone,

and lithic-dacitic tuff; (2) the middle section consists of flysch, felsic fine-grained tuff, tuffaceous siltstone, tuffaceous sandstone, sandstone, and mudstone; (3) and the uppermost sequence comprises tuffaceous sandstone interbedded with small amounts of tuffaceous siltstone, tuffaceous mudstone, and lithic tuffs [26]. These sequences are invaded by late Carboniferous–early Permian granitic plutons, gabbroic-dioritic dikes, and dioritic stocks and porphyries [27–30].

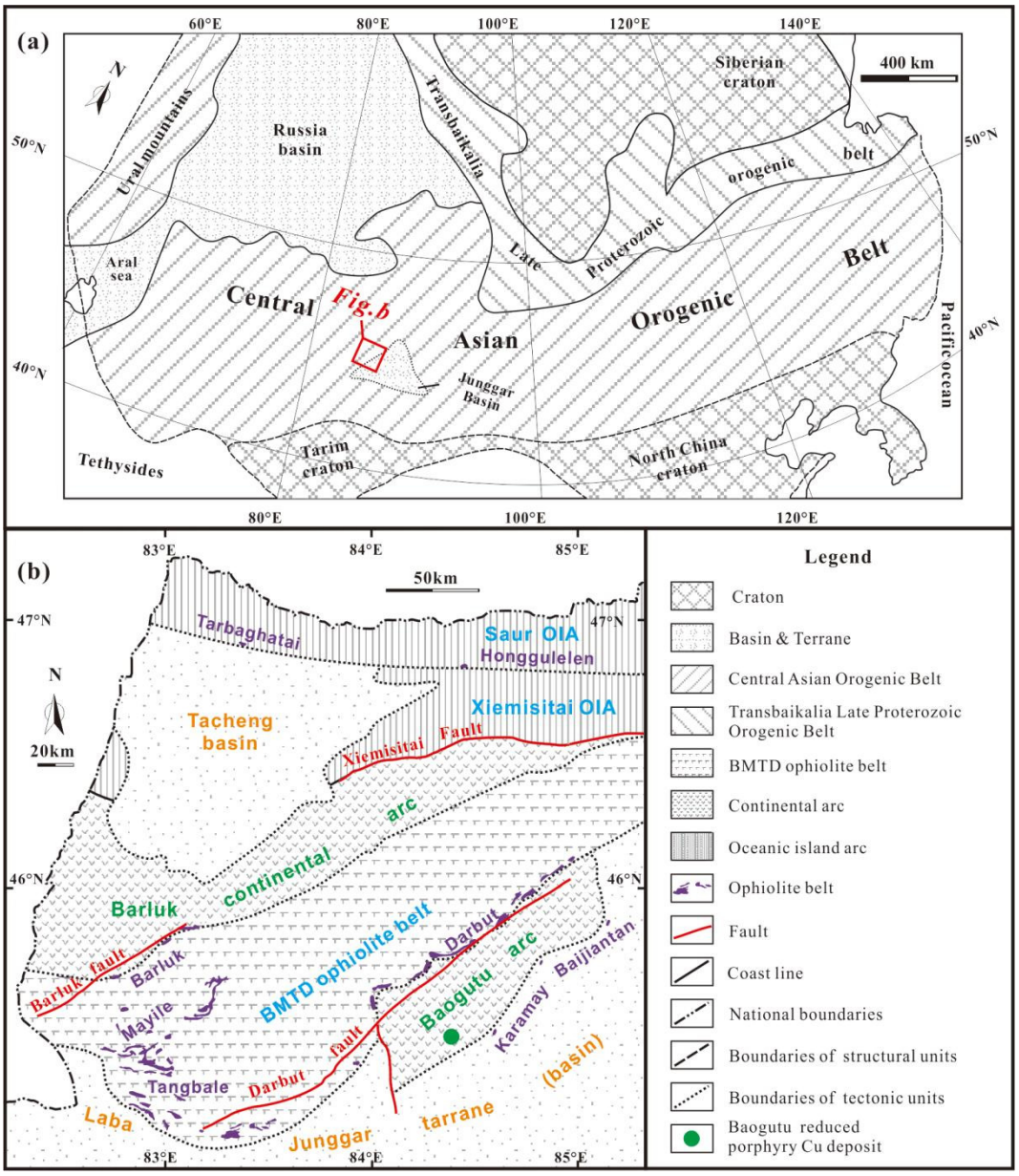

Figure 1. Location (**a**), (revised from [16,17]) and tectonic units (**b**), (revised from [19,20]) of the West Junggar, CAOB. Abbreviations: BMTD: Barluk–Mayile–Tangbale–Darbut; OIA: oceanic island arc.

2.2. Intrusive Complex

The Baogutu reduced Cu porphyry-type deposit is situated in the southeastern part of the Baogutu arc, hosted by a 0.6 km^2 shallow felsic intrusion named the Baogutu V stock (Figure 2a). It is composed of calc-alkaline magmatic rocks, e.g., diorites, granite porphyries, and porphyritic diorites [7,10,27,28]. Dioritic and granite porphyries are the main ore-bearing intrusive phase and are emplaced into the early Carboniferous fine-grained tuff, tuffaceous siltstone, and sandstone. The porphyritic diorite dikes intruded

into the earlier felsic (diorites and granite porphyries) stock and tuffaceous country-rock. Moreover, Cu-bearing gabbro occurs at a depth of 550–650 m in the dioritic stock [20].

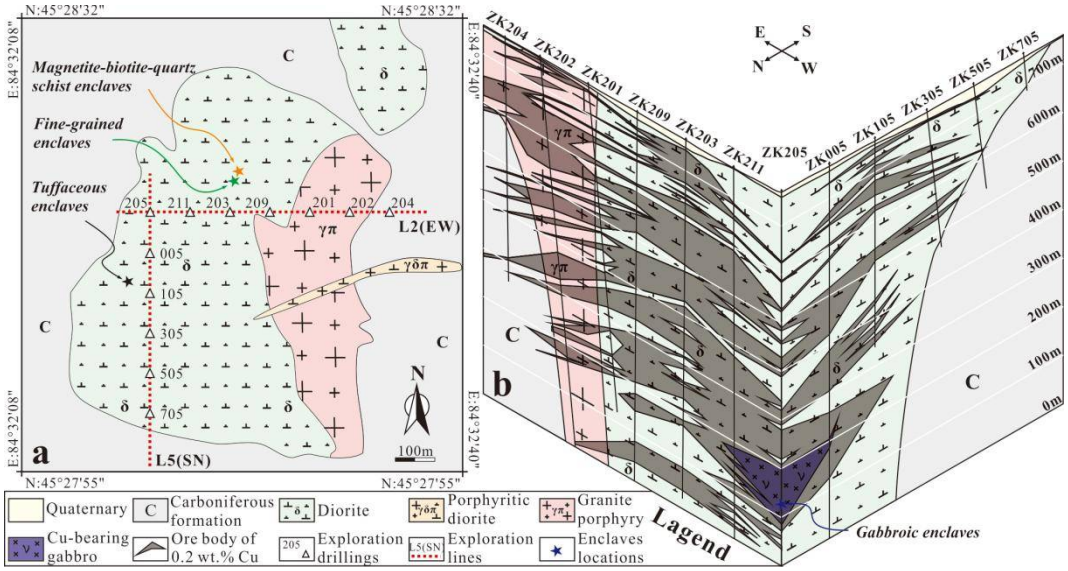

Figure 2. Geological map (**a**) and an EW–NS joint cross-section (**b**) of the Baogutu reduced Cu porphyry-type deposit (modified according to [7,20]).

2.3. Alteration

Ca–Na silicate, potassic, propylitic, and sericitic alterations are preserved in the Baogutu reduced Cu porphyry-type deposit. Ca–Na silicate alteration occurred earlier than the main stage of sulfide mineralization, which is characterized by actinolite, albite, magnetite, and epidote association, mainly in the diorites [7,28]. Potassic alteration was widely distributed in diorites, granite porphyries, and porphyritic diorites, which has been associated with the Cu mineralization. Secondary biotite + potassic feldspar assemblages are concentrated in the inner zone and epidote + chlorite in the outer zone, and these two zones are accompanied by simultaneously or subsequently other propylitization, e.g., calcitization, actinolitization, and pyritization [7]. The sericitic alteration overprints the potassic and propylitic alterations in diorites and granite porphyries, as demonstrated by a sericite+ quartz+ carbonate+ pyrite assemblage [28].

2.4. Mineralization

The Baogutu reduced Cu porphyry-type deposit contains 63×10^4 t of Cu with average grade of 0.28 wt.%, 1.8×10^4 t of Mo with an average grade of 0.011 wt.%, and 14 t of Au with average grade of 0.1 g/t [7]. The mineralized intrusive complex at Baogutu contains a predominance of disseminated Cu-Mo-Au mineralization together with lesser amounts of vein- (>1 cm wide), veinlet- (<1 cm wide), and breccia-hosted mineralization, which is found in diorites, granite porphyries, and tuffaceous country-rocks. Cu-Au mineralization is localized in the main parts of the complex and at its outer contacts [28]. The ore minerals are chalcopyrite, pyrrhotite, pyrite, molybdenite, and gold, with subordinate arsenopyrite, bornite, galena, sphalerite, ilmenite, and titanomagnetite. The gangue minerals are mainly composed of biotite, potassic feldspar, sericite, amphibole, epidote, chlorite, calcite, sphene, zeolite, and quartz [7,28]. The Cu ore body is delineated within a 0.2 wt.% Cu shell in an EW–NS joint cross-section (Figure 2b), together with multiple thick plates in a funnel shape [7] distributed in the diorites and granite porphyries.

3. Enclave Petrography

Four types of enclaves were defined in this study: a gabbroic enclave (Type 1), a schist enclave (Type 2), a fine-grained dioritic enclave (Type 3), and a tuffaceous siltstone enclave (Type 4). Detailed descriptions of these enclaves are provided in the following.

The biggest gabbroic enclave (Type 1) was identified in drilling cores at a depth of 550–650 m within the dioritic stock in the Baogutu deposit (Figure 3a,b). Some smaller sized (10–50 mm) gabbroic enclaves were also preserved in the host diorites (Figure 3c,d). These gabbroic enclaves mainly consist of 10–4000 μm diopside (>50 vol.%), 10–2000 μm plagioclase (40 vol.%), and 10–150 μm hornblende (~5 vol.%). The plagioclase phenocrysts have columnar-shaped, polysynthetic twins, polysynthetic twins, and high elongation ratios from 3 to 8. Parts of the euhedral relicts of the diopside glomerocrysts are fragmented (Figure 3b,d). More importantly, the gabbroic enclaves contain highly concentrated Cu (>1000 ppm), which occurs as chalcopyrite grains in intracrystalline cracks or along the boundaries of plagioclase and diopside phenocrysts [20].

Schist enclaves (Type 2) with a size of 20–100 mm (Figure 3e) occur in the diorites. These enclaves are irregularly rounded and mainly consist of quartz (>60 vol.%, 10–80 μm), biotite (~20 vol.%, 10–400 μm), and magnetite (~15 vol.%, 10–50 μm). The characteristics of layered minerals, folded bedding structures, and parallel foliations (Figure 3f,g) [18] indicate that they are typical schist enclaves. Additionally, the mineral composition and layered structural feature of these schist enclaves are consistent with metamorphosed (greenschist to amphibolite facies) sedimentary/volcanic rocks that were reported in the southern Laba–Junggar terrane by Buckman and Aitchison [31].

The fine-grained dioritic enclaves (Type 3) were previously identified as felsic microgranular or fine-grained enclaves by Shen and Pan [8] and Wu et al. [20]. They were widely distributed in diorites with irregular circular or elliptical shapes (Figure 4a). These enclaves are 10–30 mm in width and have either sharp or diffuse boundaries with their host diorites. These enclaves consist of fine-grained, 200 to 800 μm plagioclase (60–70 vol.%), 100 to 600 μm hornblende (10–15 vol.%), 50 to 400 μm biotite (10–15 vol.%), and 20 to 200 μm quartz (5–8 vol.%) (Figure 4b). The accessory minerals include apatite, zircon, ilmenite, magnetite, pyrrhotite, pyrite, and chalcopyrite [20].

Tuffaceous siltstone enclaves (Type 4) were identified in Baogutu diorites in this study. Most are preserved as irregularly round or elliptical in the diorites. They are 20–100 mm in size (Figure 4c). The mineral assemblage includes 20–200 μm biotite (>30 vol.%), 20–30 μm quartz (~25 vol.%), 20–30 μm plagioclase (~25 vol. %), and minor accessory minerals (~5 vol.%, include: apatite, zircon, ilmenite, magnetite, pyrite, etc.) (Figure 4d). These tuffaceous siltstone enclaves underwent silicification and potassic alteration (biotitization).

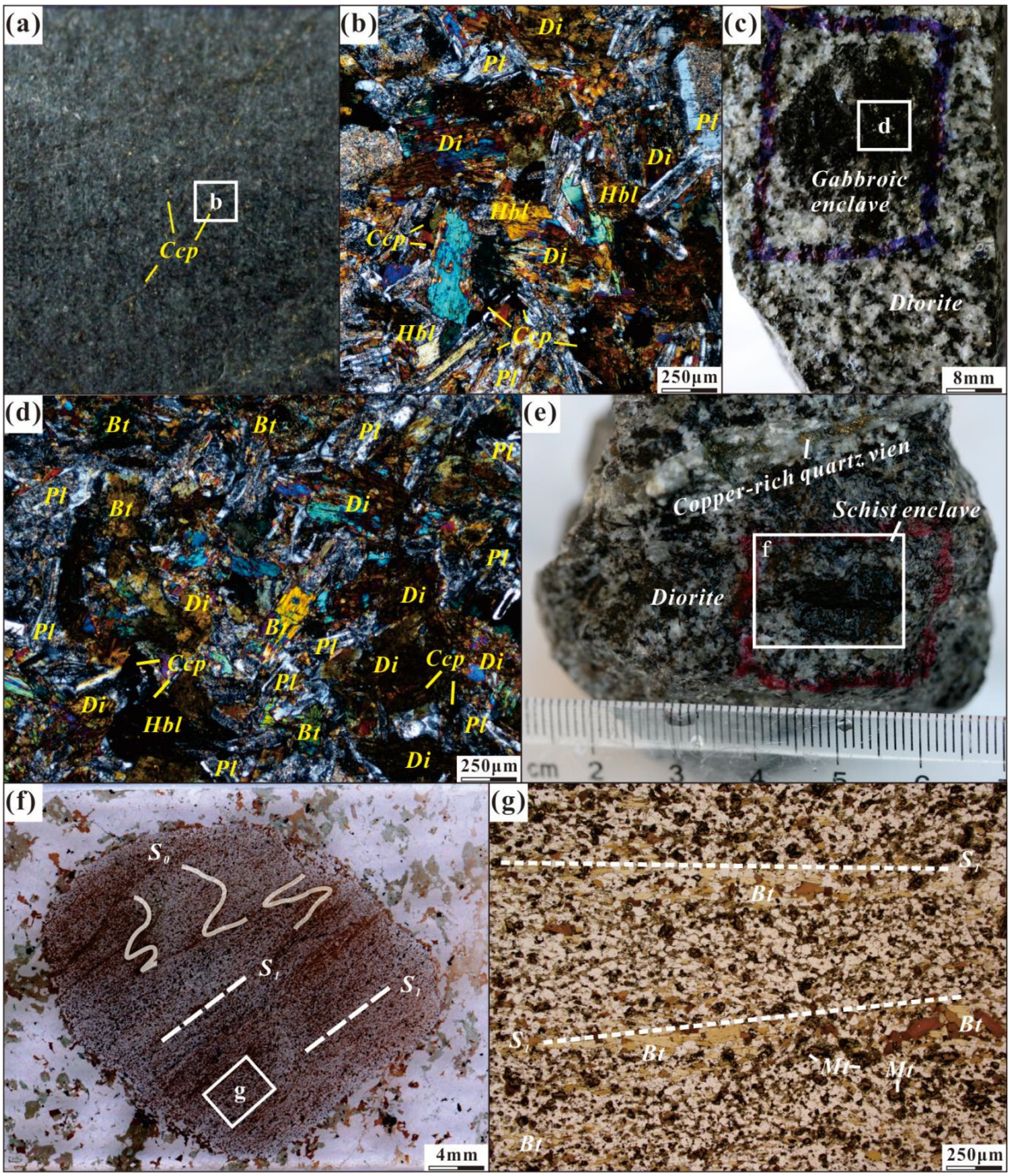

Figure 3. Representative photographs of the gabbroic enclave and schist enclave within diorite. Hand specimen of the bulky gabbroic enclave (**a**); photomicrograph of the bulky gabbroic enclave (**b**); hand specimen of diorite with a smaller gabbroic enclave (**c**); photomicrograph of the smaller gabbroic enclave (**d**); diorite specimen containing a schist enclave (**e**); scanning image showing the outer morphology and inner deformation of the schist enclave (**f**); a parallel light microphotography of the deformed schist enclave (**g**). The white line in panel f represents the bedding structure (S_0), and the white dashed line in panels f and g represent foliations (S1) displayed by oriented quartz and biotite crystals. Abbreviation: Bt: biotite; Ccp: chalcopyrite; Di: diopside; Hbl: hornblende; Mt: magnetite; Pl: plagioclase.

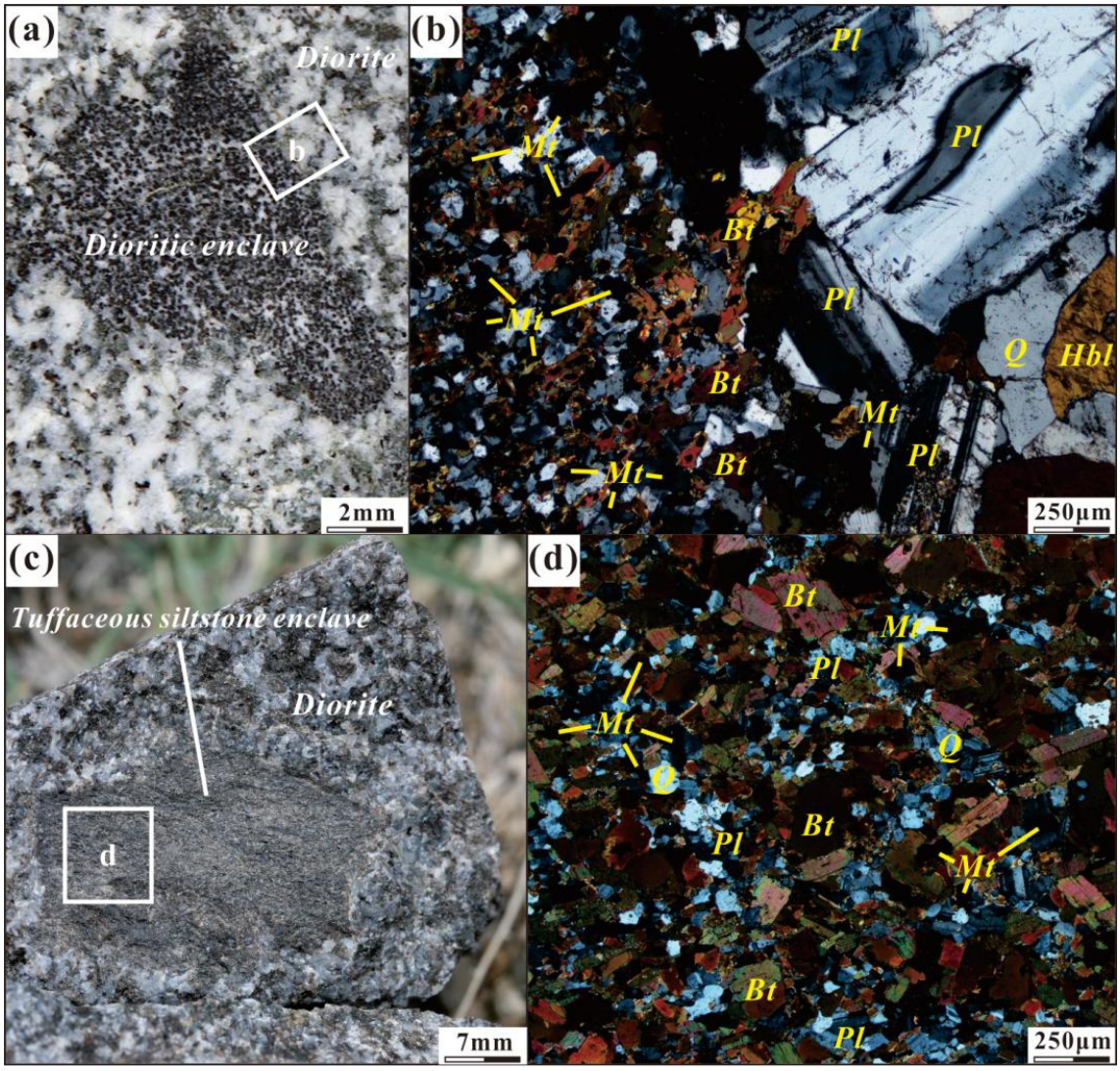

Figure 4. Representative field photographs and micrographs under cross-polarized light of the fine-grained dioritic enclave (**a**,**b**) and tuffaceous siltstone enclave (**c**,**d**) hosted in diorite. Abbreviation: Bt: biotite; Hbl: hornblende; Pl: plagioclase; Q: quartz.

4. Sample Selection and Analytical Techniques

After detailed petrographic inspection, the representative tuffaceous siltstone enclave samples, which have irregularly round or elliptical morphology, igneous texture, and felsic mineral composition from the Baogutu reduced Cu porphyry-type deposit, were selected for zircon U-Pb dating using secondary ion mass spectrometry (SIMS). These samples were crushed and powdered in an agate mill. The analyses were conducted at the Institute of Geology and Geophysics, the Chinese Academy of Sciences (IGGCAS).

Zircon grains were separated using conventional heavy fraction and magnetic techniques. Representative zircon grains from tuffaceous siltstone enclave samples, together with zircon standard 91500, were mounted in epoxy mounts, which were then polished for analysis. All mounted zircons were documented in transmitted and reflected light (micro) photographs and cathodoluminescence (CL) images in order to reveal their internal structures. The mounts were vacuum-coated with high-purity gold prior to SIMS analysis.

Measurements of U, Th, and Pb were conducted using the Cameca IMS–1280 SIMS. U-Th-Pb ratios and absolute abundances were determined relative to the standard zircon 91500 [32], the analyses of which were interspersed with those of unknown grains, using operating and data-processing procedures similar to those described by Li et al. [33].

A long-term uncertainty of 1.5% (1 RSD) for $^{206}Pb/^{238}U$ measurements of the standard zircons was propagated to the unknowns [34], although the measured $^{206}Pb/^{238}U$ error in a specific session is generally around 1% (1 RSD) or less. The measured compositions were corrected for common Pb using non-radiogenic ^{204}Pb. Corrections are sufficiently small to be insensitive to the choice of common Pb composition, and an average of present-day crustal composition [35] is used for the common Pb, assuming that the common Pb is largely surface contamination introduced during sample preparation. Uncertainties in individual analyses in data tables are reported at a 1σ level; mean ages for pooled U/Pb (and Pb/Pb) analyses are quoted with the 95% confidence interval. Data reductions were carried out using the Isoplot/Ex program version 2.49 [36]. Errors quoted as age dates are at the 1σ levels. Zircon U-Pb results are presented in Table 1.

Table 1. SIMS zircon U-Pb ages of the tuffaceous siltstone enclaves in the Baogutu reduced Cu porphyry-type deposit, West Junggar, Northwest China.

Sample No.	Content/10^{-6}		Th/U	$^{207}Pb/^{206}Pb$		$^{207}Pb/^{235}U$		$^{206}Pb/^{238}U$		$^{207}Pb/^{206}Pb$		$^{207}Pb/^{235}U$		$^{206}Pb/^{238}U$		f_{206}%
	Th	U		Ratio	±σ	Ratio	±σ	Ratio	±σ	Age/Ma	±σ	Age/Ma	±σ	Age/Ma	±σ	
13BGT04-B@1	111	134	0.8	0.38535	2.56	0.05359	1.67	0.05220	1.94	353.9	37.3	327.7	6.2	331.0	7.3	{0.18}
13BGT04-B@3	74	179	0.4	0.41073	3.78	0.05217	3.38	0.05710	1.70	292.7	75.3	358.0	5.9	349.4	11.2	{0.83}
13BGT04-B@4	282	232	1.2	0.41216	2.69	0.05322	1.50	0.05620	2.24	338.1	33.5	352.3	7.7	350.4	8.0	{0.00}
13BGT04-B@5	65	92	0.7	0.37791	3.46	0.05331	2.65	0.05140	2.22	342.2	58.9	323.2	7.0	325.5	9.7	{0.23}
13BGT04-B@7	343	266	1.3	0.40419	2.56	0.05408	1.25	0.05420	2.24	374.6	28.0	340.3	7.4	344.7	7.5	{0.38}
13BGT04-B@8	***35***	***98***	***0.4***	***13.30594***	***2.49***	***0.18423***	***0.74***	***0.52380***	***2.38***	***2691.3***	***12.3***	***2715.4***	***52.9***	***2701.6***	***23.8***	***{0.02}***
13BGT04-B@9	127	164	0.8	0.40421	2.41	0.05410	1.75	0.05420	1.65	375.1	39.0	340.2	5.5	344.7	7.1	{0.59}
13BGT04-B@10	105	106	1.0	0.37627	3.18	0.05174	2.58	0.05270	1.85	273.9	58.1	331.4	6.0	324.3	8.9	{0.36}

Note: Analyses in shadow were selected for the concordia age calculation, and their cathodoluminescence (CL) images are exhibited at the bottom of Figure 5a,b. The bold italic data denote the Neoarchean zircon, the CL images of which are shown in Figure 5a.

5. Analytical Results

The zircons from the tuffaceous siltstone enclave samples are tetragonal prismatic crystals, 50–120 μm in size with elongation ratios from 1 to 3, which have an oscillatory growth zone visible in the CL images (Figure 5a,b). They have a Th/U ratio range from 0.4 to 1.3. These characteristics are in accordance with magmatic zircons [37,38]. The SIMS analysis result suggests that most of these magmatic zircons have $^{206}Pb/^{238}U$ ages from 324.3 ± 8.9 Ma to 349.4 ± 11.2 Ma and $^{207}Pb/^{235}U$ ages from 323.2 ± 7.0 Ma to 358.0 ± 5.9 Ma (Table 1). On the concordia line, they demonstrated a concordia age of 339.2 ± 7.5 Ma (MSWD = 0.55) (Figure 5b), which may represent the formation time of the protolith of the tuffaceous siltstone enclaves. This age is consistent with the 336 Ma tuffaceous country-rock but is obviously older than the 311–318 Ma host diorites [10,20]. Moreover, grain 8 is a typical Neoarchean magmatic (inherited) zircon (Figure 5a) that has a consistent isotopic age: the $^{207}Pb/^{206}Pb$ age is 2691.3 ± 12.3 Ma; the $^{206}Pb/^{238}U$ age is 2701.6 ± 23.8 Ma; and the $^{207}Pb/^{235}U$ age is 2715.4 ± 52.9 Ma.

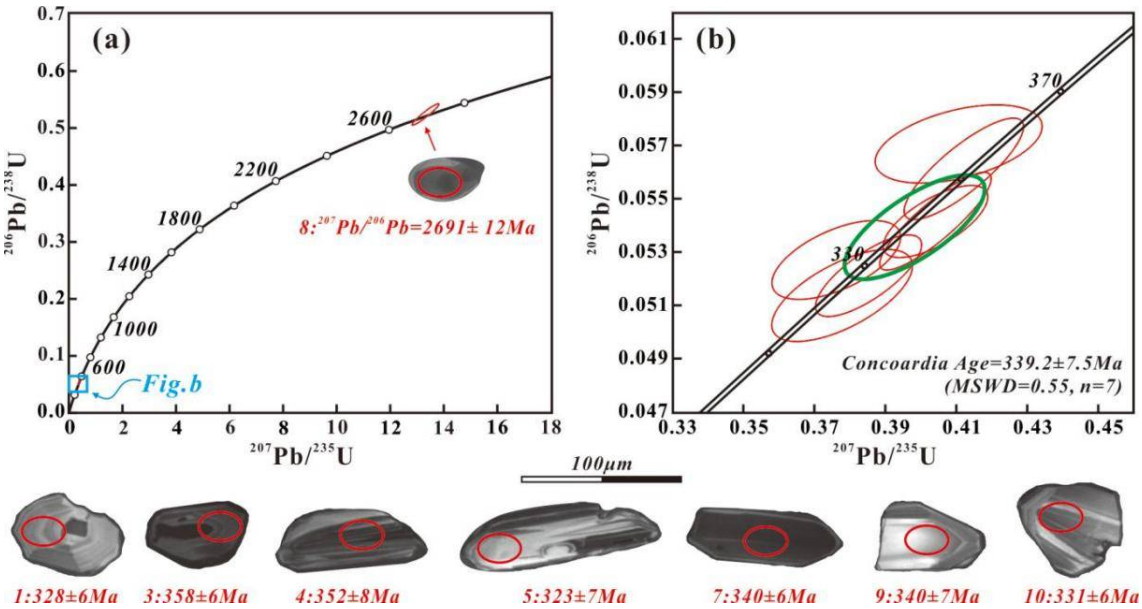

Figure 5. SIMS U-Pb concordia age diagrams (**a**,**b**) with CL photos of zircons in the tuffaceous siltstone enclaves. The solid ellipses in CL photos of zircons represent the analytical location of the U-Pb age. The number adjacent to the CL photos in Figure 5a shows the plot number (*n*) with $^{207}Pb/^{206}Pb$ age data, and the numbers under CL photos show the plot number (*n*) with $^{206}Pb/^{238}U$ age data.

6. Discussion

Enclaves in granites and volcanic rocks can provide information concerning the petrogenesis, evolution, and emplacement processes with their host rocks [39–41]. Thus, the gabbroic enclave, schist enclave, fine-grained dioritic enclave, and tuffaceous siltstone enclave were used to assess the magmatic origination and evolution of the Baogutu reduced Cu porphyry-type deposit.

6.1. Petrogenesis of the Enclaves

6.1.1. Gabbroic Enclave (Type 1)

The gabbroic enclaves are typical restites associated with the earliest intrusive phases at Baogutu, which have a U-Pb zircon age of 318.2 6 ± 0.8 Ma, low SiO_2 contents of approximately 48 wt%, and high $\varepsilon_{Hf}(t)$ values ranging from +8.82 to +14.4 [20]. The plagioclase formed around the hornblende and diopside glomerocrysts was fragmented as euhedral relicts (Figure 3b,d). This petrological evidence indicates that these minerals in the gabbroic enclaves formed as a result of a high-pressure process and decompression. Wu et al. [20] reported that the gabbroic enclaves contain 1182–1260 ppm Cu and interpreted these enclaves to be the residuals of unusually Cu-rich mantle-derived mafic magma that was incorporated into the subsequent felsic magma during the later magma-evolution process.

6.1.2. Schist Enclave (Type 2)

The layered minerals of biotite and magnetite, folded bedding structures, and parallel foliations (Figure 3f,g) illustrate that these enclaves have features in accordance with magnetite-biotite-quartz schist. We proposed that these schist enclaves are the undigested solid bodies incorporated into the magma during the partial melting process in the magma source, similar to those in the Bingham Cu porphyry-type deposit [12]. Minerals in the schist enclaves were formed in a directional parallel structure (oriented biotite, Figure 3g), suggesting that they experienced (re-)crystallization under an anisotropic stress field. The presence of magnetite mineralization and biotitization also indicates relatively high-temperature formation conditions. Thus, these schist enclaves might originate from the deformed and metamorphic basement of the Baogutu area.

6.1.3. Fine-Grained Dioritic Enclaves (Type 3)

These fine-grained dioritic enclaves have similar mineral assemblage to those of the host diorites but with smaller mineral sizes and more biotite (Figure 4a,b). Thus, we suggested that the fine-grained dioritic enclaves might be the autolith that experienced relatively rapid fractionation and crystallization [20,39]. The smaller size of the autolith indicates that they were disaggregated by flow in the magma chamber [12] and might have crystallized from the dioritic magma.

6.1.4. Tuffaceous Siltstone Enclave (Type 4)

The tuffaceous siltstone enclaves are xenoliths and could have been trapped into the magma during upwelling or the emplacement process [41,42]. They consist of fine-grained biotite, quartz, and plagioclase (Figure 4d), similar to the country-rock in composition. Moreover, the zircon age (339.2 $\pm$ 7.5 Ma) (Figure 5b) of the tuffaceous siltstone enclaves is similar to the formation age of the country-rock (336.3 $\pm$ 2.5 Ma) [43]. Thus, the tuffaceous siltstone enclaves provide convincing evidence of country-rock contamination [8].

6.2. Magma Process

6.2.1. Source Features

Previous studies have suggested that the magma of dioritic–granitic intrusions in the main Baogutu V stock was probably derived from the partial melting of residual subducted oceanic crust and juvenile mantle materials [27,44]. Cao et al. [10] further indicated that these dioritic–granitic intrusions were ilmenite-series I-type granitoids, which were also genetically related to asthenosphere mantle components. More importantly, Wu et al. proposed the possibility of mafic magma represented by gabbroic rocks [20]. He suggested that this may be the residual of early-stage unusually Cu-rich magma derived from a mixture process of metasomatized mantle wedge, the hydrous slab, and old crustal materials.

In this paper, the gabbroic enclaves (Type 1) and schist enclaves (Type 2) were distributed in the main diorite stock and were both derived from the deep magmatic source region (Figure 6a) [45]. They might be derived from the metamorphic mafic rocks and volcanic–sedimentary rocks, which reveals that the mantle and sediments (including subducted oceanic sediments and crustal materials) contribute to the magma source. This hypothesis is also supported by previous zircon $\delta^{18}O$ geochemical studies (compositions up to 7.4‰) and the $\varepsilon_{Nd}(t)$ values (up to +7.5) of the host diorites. The metamorphic volcanic–sedimentary rocks could be the strata that formed earlier in the northwest margin of the southeastern Laba–Junggar terrane (the Baogutu arc), which were deeply buried and experienced compressional deformation during the subduction process. Therefore, we propose that the magma sources of the Baogutu intrusions were formed from the mixture of partial melting of the metasomatized mantle wedge, the hydrous slab, crustal materials, and asthenosphere mantle components

6.2.2. Fractional Crystallization

The fractional crystallization process occurred in the main diorite stock according to the appearance of fine-grained dioritic enclaves and plagioclase, hornblende, biotite, and quartz phenocrysts. These autoliths have either sharp or diffuse boundaries with their host diorites, which suggests that they were part of the main phases that crystallized from the dioritic magma (Figure 6b). Moreover, fractional crystallization also impacted the precipitation of the disseminated sulfide.

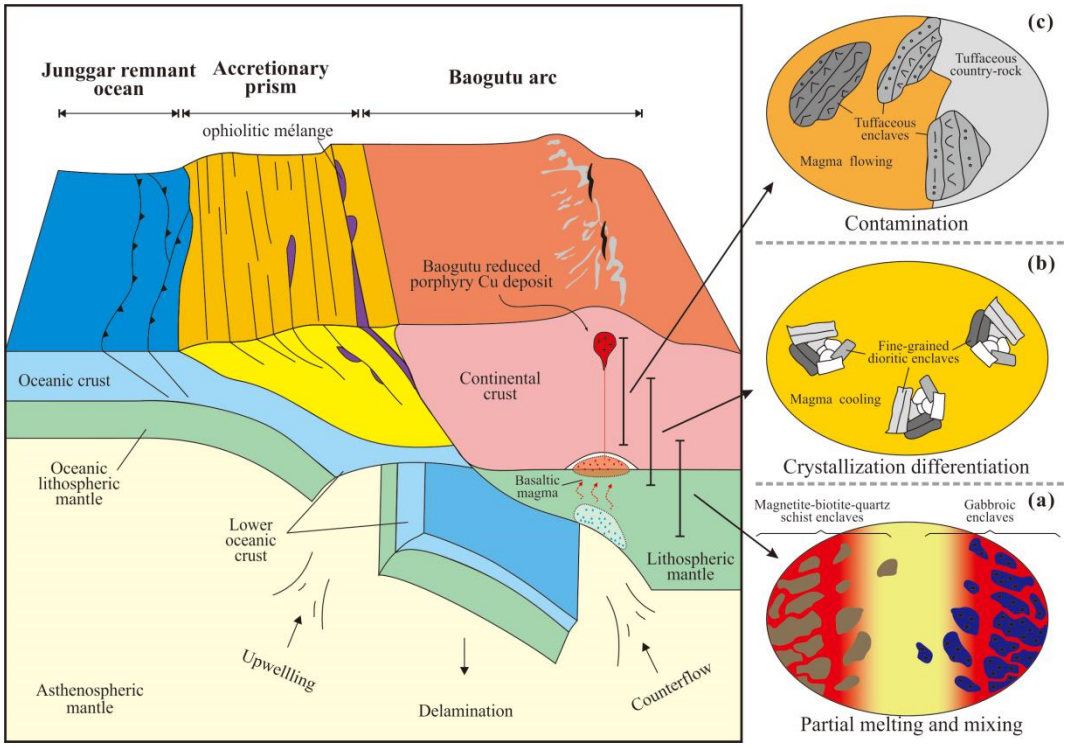

Figure 6. A simplified model to show the tectonic environment and magmatic process of the Baogutu reduced Cu porphyry-type deposit in West Junggar (modified from [45]). Panels (**a**), (**b**) and (**c**) show the multiple hypotheses of the enclaves' origins in the Baogutu reduced Cu porphyry-type deposit.

6.2.3. Contamination

Cao et al. [10] first suggested that the contamination of sediments was less than 8% in the Baogutu reduced Cu porphyry-type deposit, and the high $\delta^{18}O$ values (up to 7.4‰) of host diorites indicated a mixture of oceanic metasediments more or less. Shen and Pan [8] additionally proposed that the elemental and Sr–Nd compositions of the gabbro and diorite have a transitional relationship with the country-rocks. The tuffaceous siltstone enclaves exhibited as xenoliths in the main diorite stock further verified a significant contamination by early Carboniferous country-rock in this study. These tuffaceous siltstone enclaves might be derived from the wall rocks [12,41,42]. The debris from early Carboniferous wall rocks was enveloped into the melt during magma ascent or emplacement, inducing a typically contaminative phenomenon in the Baogutu reduced Cu porphyry-type deposit (Figure 6c). The contamination process might involve both felsic components and reduced materials (e.g., Carbonaceous sediment) to induce the chemical variation in the Baogutu rocks and promote the reduced mineralization [8].

Sillitoe [2] proposed that Cu porphyry-type systems were initiated by the injection of oxidized magma saturated with S- and metal-rich, aqueous fluids from cupolas on the tops of the subjacent parental plutons. Cao et al. [7] deduced that the reduced magmatic-hydrothermal system, which has produced the uncommon mineral assemblage (widespread hypogene and hydrothermal pyrrhotite, arsenopyrite, predominant ilmenite with trace magnetite), restricted the scale of mineralization of the Baogutu Cu deposit. The earlier reduced condition in magmatic phase induced more disseminated sulfide mineralization (e.g., hypogene pyrrhotite) in Baogutu than other Cu porphyry-type deposits. The crystallization of abundant disseminated hypogene pyrrhotite extracts large amounts of Cu [9]. Moreover, the variations in temperature, pressure, pH value, volatiles, etc., in hydrothermal fluid phase may lead to further reduced and formed vein-, veinlet-, or further disseminated sulfide mineralization accompanied by hydrothermal alterations [2]. Thus, contamination was a significant condition which might trigger the formation of the

main diorite stock and the associated mineralization of the Baogutu reduced Cu porphyry-type deposit.

Thus, the process of multiple enclaves occurring in the magma can be further divided into three stages: the source-derived gabbroic enclaves and schist enclaves were melted in the early stage (Figure 6a); the fine-grained dioritic enclaves were crystallized in the middle stage (Figure 6b); and the tuffaceous siltstone enclaves were enveloped into ascending magma in the last stage (Figure 6c).

6.3. Tectonic Implication

The discovery of schist enclaves indicates that the early Carboniferous volcano-sedimentary rocks in the Baogutu reduced Cu porphyry-type deposit have a deformed and metamorphic basement. Moreover, these early Carboniferous volcano-sedimentary rocks unconformably overlay a deformational and metamorphic zone, which is likely related to a collision zone that was formed during the closure of the Junggar Ocean [18]. In addition, the newly discovered 2691.3 ± 12.3 Ma inherited zircon in the tuffaceous siltstone enclaves may imply that the Baogutu arc has an Archean basement. This Archean basement has probably contributed to the formation of Baogutu host diorites, although this deduction has not been confirmed by other geochemical studies. This old zircon grain with an euhedral morphology, oscillatory zoning, and a Th/U ratio of 0.4 is attributed to typical magmatic or inherited magmatic zircons [18,37]. The consistent isotopic ages, e.g., the $^{207}Pb/^{206}Pb$ age is 2691.3 ± 12.3 Ma, the $^{206}Pb/^{238}U$ age is 2701.6 ± 23.8 Ma, and the $^{207}Pb/^{235}U$ age is 2715.4 ± 52.9 Ma, not only indicate the zircon formation age, but also reflect the source age.

Furthermore, previous geochronological, geochemical, and tectonic studies reported that the following: (1) abundant Neoproterozoic–Neoarchean (1.88–2.54 Ga) magmatic zircons occur in the basalts of the Karamay area in the Baogutu arc [46]; (2) igneous rocks in the Baogutu area mainly belong to calc–alkaline series and are characterized by an enrichment of Zr and Hf [20]; and (3) the southern part of the Junggar Basin possibly has a Precambrian basement [23]. This evidence further indicates that the igneous rocks in the Baogutu arc were probably formed in a continental island arc setting (such as the East Java, Solomon, Japan, and Taiwan arc [18,47–50]; Figure 6a–c).

7. Conclusions

Four types of enclaves were identified in the Baogutu reduced PCD. The gabbroic enclaves (Type 1) and schist enclaves (Type 2) could be restites and immiscible enclaves, respectively, formed in the magma source. The tuffaceous siltstone enclaves (Type 3) present as xenoliths formed during magmatic migration, whereas the fine-grained dioritic enclaves (Type 4) are likely to be autoliths derived from inhomogeneity fractional crystallization in magmatic evolution.

The concordia zircon U-Pb age of tuffaceous siltstone enclaves was found to be 339.2 ± 7.5 Ma (MSWD = 0.55) based on the SIMS test. These tuffaceous siltstone enclaves may be derived from the Late Carboniferous country-rock, and further confirmed the country-rock contamination of magmas.

The magma of Baogutu intrusive rocks is dominantly derived from the mixing of the partially melted metasomatized mantle wedge, the hydrous slab, crustal materials, and asthenosphere mantle components. Fractional crystallization and contamination may have occurred during the upwelling or emplacement of magma.

The Baogutu arc, which produced these granitoids and enclaves, was probably a continental arc.

Author Contributions: C.W. and T.H. conceived the presented idea. C.W. and T.H. carried out the experiment. All authors, C.W., T.H., X.-W.X., X.Z., C.-X.W., W.-J.L., K.-F.S., H.-J.Z., B.W. and L.-H.D., discussed the results and contributed to the final manuscript. All authors have read and agreed to the published version of the manuscript.

Funding: This research was jointly supported by the National Natural Science Foundation of China (41802093); the National Key R&D Program of China (2017YFC0601201 and 2018YFC0604002); the Project of Xinjiang Bureau of Geology and Mineral Resources (2011BAB06B03-3); the Project of Development and Research Center of China Geology Survey (DD20190405 and DD20190406) of China; and the Fundamental Research Funds for the Central Universities, Sun Yat-sen University (2021qntd23).

Acknowledgments: We would like to thank Hao Li, Qiang Ke, and Hang Li for their support during the field work and for their professional input. Moreover, the first author wants to thank his wife Yan Liu and child Pei-zhou Wu for their encouragement.

Conflicts of Interest: The authors declare no conflict of interest.

References

1. Seedorff, E.; Dilles, J.H.; John, M.; Proffett, J.; Einaudi, M.T.; Zurcher, L.; Stavast, W.J.A.; Johnson, D.A.; Barton, M.D. Porphyry deposits: Charcteristics and origin of hypogene features. In *Economic Geology One Hundredth Anniversary Volume 1905–2005*; Hedenquist, J.W., Thompson, J.F.H., Goldfarb, R.J., Richards, J.P., Eds.; Society of Economic Geologists: Littleton, CO, USA, 2005; pp. 251–298.
2. Sillitoe, R.H. Porphyry copper systems. *Econ. Geol.* **2010**, *105*, 3–41. [CrossRef]
3. Xu, X.W.; Li, H.; Peters, S.G.; Qin, K.Z.; Mao, Q.; Wu, Q.; Hong, T.; Wu, C.; Liang, G.L.; Zhang, Z.F.; et al. Cu-rich porphyry magmas produced by fractional crystallization of oxidized fertile basaltic magmas (Sangnan, East Junggar, PR China). *Ore Geol. Rev.* **2017**, *91*, 296–315. [CrossRef]
4. Wang, Y.H.; Zhang, F.F.; Xue, C.J.; Liu, J.J.; Zhang, Z.C.; Sun, M. Geology and Genesis of the Tuwu Porphyry Cu Deposit, Xinjiang, Northwest China. Economic Geology. *Econ. Geol.* **2021**, *116*, 471–500. [CrossRef]
5. Hong, T.; Xu, X.W.; Gao, J.; Peters, S.G.; Zhang, D.; Jielili, R.; Xiang, P.; Li, H.; Wu, C.; You, J.; et al. Ore-forming adakitic porphyry produced by fractional crystallization of oxidized basaltic magmas in a subcrustal chamber (Jiamate, East Junggar, NW China). *Lithos* **2018**, *296*, 96–112. [CrossRef]
6. Hedenquist, J.W.; Lowenstern, J.B. The role of magmas in the formation of hydrothermal ore deposits. *Nature* **1994**, *370*, 519–527. [CrossRef]
7. Cao, M.J.; Qin, K.Z.; Li, G.M.; Jin, L.Y.; Evans, N.J.; Yang, X.R. Baogutu: An example of reduced porphyry Cu deposit in western Junggar. *Ore Geol. Rev.* **2014**, *56*, 159–180. [CrossRef]
8. Shen, P.; Pan, H.D. Country-rock contamination of magmas associated with the Baogutu porphyry Cu deposit, Xinjiang, China. *Lithos* **2013**, *177*, 451–469. [CrossRef]
9. Cao, M.J.; Qin, K.Z.; Li, G.M.; Yang, Y.H.; Evans, N.J.; Zhang, R.; Jin, L.Y. Magmatic process recorded in plagioclase at the Baogutu reduced porphyry Cu deposit, western Junggar, NW-China. *J. Asian Earth Sci.* **2014**, *82*, 136–150. [CrossRef]
10. Cao, M.J.; Qin, K.Z.; Li, G.M.; Evans, N.J.; Hollings, P.; Jin, L.Y. Genesis of ilmenite series I-type granitoids at the Baogutu reduced porphyry Cu deposit, western Junggar, NW-China. *Lithos* **2016**, *246*, 13–30. [CrossRef]
11. Cao, M.J.; Qin, K.Z.; Li, G.M.; Evans, N.J.; Jin, L.Y. Abiogenic Fischer–Tropsch synthesis of methane at the Baogutu reduced porphyry copper deposit, western Junggar, NW-China. *Geochim. Cosmochim. Acta* **2014**, *141*, 179–198. [CrossRef]
12. Core, D.P.; Kesler, S.E.; Essene, E.J. Unusually Cu-rich magmas associated with giant porphyry copper deposits: Evidence from Bingham, Utah. *Geology* **2006**, *34*, 41–44. [CrossRef]
13. Wu, S.; Zheng, Y.Y.; Sun, X.; Liu, S.A.; Geng, R.R.; You, Z.M.; Ouyang, H.T.; Lei, D.; Zhao, Z.Y. Origin of the Miocene porphyries and their mafic microgranular enclaves from Dabu porphyry Cu-Mo deposit, southern Tibet: Implications for magma mixing/mingling and mineralization. *Int. Geol. Rev.* **2014**, *56*, 571–595. [CrossRef]
14. Zhao, X.B.; Xue, C.J.; Symons, D.T.A.; Zhang, Z.C.; Wang, H.G. Microgranular enclaves in island-arc andesites: A possible link between known epithermal Au and potential porphyry Cu–Au deposits in the Tulasu ore cluster, western Tianshan, Xinjiang, China. *J. Asian Earth Sci.* **2014**, *85*, 210–223. [CrossRef]
15. Zhang, F.F.; Wang, Y.H.; Liu, J.J.; Xue, C.J.; Wang, J.P.; Zhang, W.; Li, Y.Y. Paleozoic Magmatism and Mineralization Potential of the Sanchakou Copper Deposit, Eastern Tianshan, Northwest China: Insights from Geochronology, Mineral Chemistry, and Isotopes. *Econ. Geol.* **2022**, *117*, 165–194. [CrossRef]
16. Sengör, A.M.C.; Natal'in, B.A. Paleotectonics of Asia: Fragments of a synthesis. In *The Tectonic Evolution of Asia*; Yin, A., Harrison, M., Eds.; Cambridge University Press: Rubey Colloquium, Cambridge, UK, 1996; pp. 486–640.
17. Windley, B.F.; Alexeiev, D.; Xiao, W.J.; Kroner, A.; Badarch, G. Tectonic models for accretion of the Central Asian Orogenic Belt. *J. Geol. Soc. Lond.* **2007**, *164*, 31–47. [CrossRef]
18. Xu, X.W.; Jiang, N.; Li, X.H.; Wu, C.; Qu, X.; Zhou, G.; Dong, L.H. Spatial-temporal framework for the closure of the Junggar Ocean in Central Asia: New SIMS zircon U-Pb ages of the ophiolitic mélange and collisional igneous rocks in the Zhifang area, East Junggar. *J. Asian Earth Sci.* **2015**, *111*, 470–491. [CrossRef]
19. Wu, C.; Hong, T.; Xu, X.W.; Cao, M.J.; Li, H.; Zhang, G.L.; You, J.; Ke, Q.; Dong, L.H. Tectonic evolution of the Paleozoic Barluk continental arc, West Junggar, NW China. *J. Asian Earth Sci.* **2018**, *160*, 48–66. [CrossRef]

20. Wu, C.; Hong, T.; Xu, X.W.; Cao, M.J.; Li, H.; Ke, Q.; Li, H.; Dong, L.H. Constraints on the formation of the Baogutu reduced porphyry copper deposit (West Junggar, NW China): Assessing the role of mafic magmas in mineralization. *Lithos* **2019**, *336*, 112–124. [CrossRef]
21. Xu, X.W.; Jiang, N.; Li, X.H.; Qu, X.; Yang, Y.H.; Mao, Q.; Wu, Q.; Zhang, Y.; Dong, L.H. Tectonic evolution of the East Junggar terrane: Evidence from the Taheir tectonic window, Xinjiang, China. *Gondwana Res.* **2013**, *24*, 578–600. [CrossRef]
22. Zhu, Y.F.; Chen, B.; Xu, X.; Qiu, T.; An, F. A new geological map of the western Junggar, north Xinjiang (NW China): Implications for Paleoenvironmental reconstruction. *Episodes* **2013**, *36*, 205–220. [CrossRef]
23. Wu, C.; Hong, T.; Xu, X.W.; Li, H.; Ke, Q.; Li, H.; Dong, L.H. Constraints on the nature of the basement of the Junggar terrane indicated by the Laba Ordovician continental arc. *Int. Geol. Rev.* **2020**, *62*, 29–52. [CrossRef]
24. Jian, P.; Liu, D.Y.; Shi, Y.R.; Zhang, F.Q. SHRIMP dating of SSZ ophiolites from northern Xinjiang Province, China: Implications for generation of oceanic crust in the Central Asian Orogenic Belt. In *Structural and Tectonic Correlation across the Central Asia Orogenic Collage: North-Eastern Segment*; Sklyarov, E.V., Ed.; Guidebook and Abstract Volume of the Siberian Workshop IGCP-480; IEC SB RAS: Irkutsk, Russia, 2005; p. 246.
25. Yang, G.X.; Li, Y.J.; Santosh, M.; Yang, B.K.; Yan, J.; Zhang, B.; Tong, L.L. Geochronology and geochemistry of basaltic rocks from the Sartuohai ophiolitic mélange, NW China: Implications for a Devonian mantle plume within the Junggar Ocean. *J. Asian Earth Sci.* **2012**, *59*, 141–155. [CrossRef]
26. An, F.; Zhu, Y.F. SHRIMP U-Pb zircon ages of tuff in Baogutu Formation and their geological significances. *Acta Petrol. Sin.* **2009**, *25*, 1437–1445, (In Chinese with English Abstract).
27. Tang, G.J.; Wang, Q.; Zhao, Z.H.; Derek, A.W.; Chen, H.H.; Jia, X.H.; Jiang, Z.Q. Geochronology and geochemistry of the Ore-bearing porphyries in the Baogutu Area (Western Junggar): Petrogenesis and their implications for tectonics and Cu-Au mineralization. *Earth Sci. J. China Univ. Geosci.* **2009**, *34*, 56–74, (In Chinese with English Abstract).
28. Shen, P.; Shen, Y.C.; Pan, H.D.; Wang, J.B.; Zhang, R.; Zhang, Y.X. Baogutu porphyry Cu-Mo-Au deposit, West Junggar, Northwest China: Petrology, alteration, and mineralization. *Econ. Geol.* **2010**, *105*, 947–970. [CrossRef]
29. Yin, J.Y.; Long, X.P.; Yuan, C.; Sun, M.; Zhao, G.C.; Geng, H.Y. A Late Carboniferous slab window: Geochronological and geochemical evidence from mafic to intermediate dykes in West Junggar, NW China. *Lithos* **2013**, *175*, 146–162. [CrossRef]
30. Yin, J.Y.; Chen, W.; Xiao, W.J.; Yuan, C.; Sun, M.; Tang, G.J.; Yu, S.; Long, X.P.; Cai, K.D.; Geng, H.Y.; et al. Petrogenesis of Early-Permian sanukitoids from West Junggar, Northwest China: Implications for Late Paleozoic crustal growth in Central Asia. *Tectonophysics* **2015**, *662*, 385–397. [CrossRef]
31. Buckman, S.; Aitchison, J.C. Tectonic evolution of Palaeozoic terranes in West Junggar, Xinjiang, NW China. In *Aspects of the Tectonic Evolution of China*; Malpas, J., Fletcher, C.J.N., Ali, J.R., Aitchison, J.C., Eds.; Geological Society of London Special Publications: London, UK, 2004; Volume 226, pp. 101–129.
32. Wiedenbeck, M.; Alle, P.; Corfu, F.; Griffin, W.L.; Meier, M.; Oberli, F.; Vonquadt, A.; Roddick, J.C.; Speigel, W. Three natural zircon standards for U-Th-Pb, Lu-Hf, trace-element and REE analyses. *Geostand. Newsl.* **1995**, *19*, 1–23. [CrossRef]
33. Li, X.H.; Liu, Y.; Li, Q.L.; Guo, C.H.; Chamberlain, K.R. Precise determination of Phanerozoic zircon Pb/Pb age by multicollector SIMS without external standardization. *Geochem. Geophy. Geosy.* **2009**, *10*, Q04010. [CrossRef]
34. Li, Q.L.; Li, X.H.; Liu, Y.; Tang, G.Q.; Yang, J.H.; Zhu, W.G. Precise U-Pb and Pb-Pb dating of Phanerozoic baddeleyite by SIMS with oxygen flooding technique. *J. Anal. At. Spectrom.* **2010**, *25*, 1107–1113. [CrossRef]
35. Stacey, J.S.; Kramers, J.D. Approximation of terrestrial lead isotope evolution by a two-stage model. *Earth Planet. Sci. Lett.* **1975**, *26*, 207–221. [CrossRef]
36. Ludwig, K.R. *SQUID 1.02: A User's Manual*; Special Publication 2; Berkeley Geochronology Center: Berkeley, CA, USA, 2001; pp. 1–19.
37. Corfu, F.; Hanchar, J.M.; Hoskin, P.W.O.; Kinny, P. Atlas of zircon textures. *Rev. Mineral. Geochem.* **2003**, *53*, 469–500. [CrossRef]
38. Hoskin, P.W.O.; Black, L.P. Metamorphic zircon formation by solid-state recrystallization of protolith igneous zircon. *J. Metamorph. Geol.* **2000**, *18*, 423–439. [CrossRef]
39. Didier, J. Granites and their enclaves. In *Developments in Petrology*; Elsevier: Amsterdam, The Netherlands, 1973; p. 393.
40. Didier, J.; Barbarin, B. Enclaves and granite petrology. In *Developments in Petrology*; Elsevier: Amsterdam, The Netherlands, 1991; p. 625.
41. Mass, R.; Nicholls, I.A.; Legg, C. Igneous and metamorphic enclaves in the S-type Deddick granodiorite, Lachlan fold belt, SE Australia: Petrographic, geochemical and Nd–Sr isotopic evidence for crustal melting and magma mixing. *J. Pet.* **1997**, *38*, 815–841. [CrossRef]
42. Bouloton, J.; Gasquet, D. Melting and undercooled crystalisation of felsic xenoliths from minor intrusions (Jebilet massif, Morocco). *Lithos* **1995**, *35*, 201–219. [CrossRef]
43. Guo, L.S.; Liu, Y.L.; Wang, Z.H.; Song, D.; Xu, F.J.; Su, L. The zircon U-Pb LA-ICP-MS geochronology of volcanic rocks in Baogutu areas, western Junggar. *Acta Petrol. Sin.* **2010**, *26*, 471–477, (In Chinese with English Abstract).
44. Shen, P.; Shen, Y.C.; Liu, T.B.; Meng, L.; Dai, H.W.; Yang, Y.H. Geochemical signature of porphyries in the Baogutu porphyry copper belt, western Junggar, NW China. *Gondwana Res.* **2009**, *16*, 227–242. [CrossRef]
45. Wu, C.; Hong, T.; Xu, X.W.; Wang, C.X.; Dong, L.H. A-type granites induced by a breaking-off and delamination of the subducted Junggar oceanic plate, West Junggar, Northwest China. *China Geol.* **2021**, *4*, 1–18. [CrossRef]

46. Zhu, Y.F.; Xu, X.; Wei, S.N.; Song, B.; Guo, X. Geochemistry and tectonic significance of OIB-type pillow basalts in western Mts. of Karamay city (western Junggar), NW China. *Acta Petrol. Sin.* **2007**, *23*, 1739–1748, (In Chinese with English Abstract).
47. Bailey, J.C. Geochemical criteria for a refined tectonic discrimination of orogenic andesites. *Chemi. Geol.* **1981**, *32*, 139–154. [CrossRef]
48. Shao, W.Y.; Chung, S.L.; Chen, W.S.; Lee, H.Y.; Xie, L.W. Old continental zircons from a young oceanic arc, eastern Taiwan: Implications for Luzon subduction initiation and Asian accretionary orogeny. *Geology* **2015**, *43*, 479–482. [CrossRef]
49. Smyth, H.R.; Hamilton, P.J.; Hall, R.; Kinny, P.D. The deep crust beneath island arcs: Inherited zircons reveal a Gondwana continental fragment beneath East Java, Indonesia. *Earth Planet. Sci. Lett.* **2007**, *258*, 269–282. [CrossRef]
50. Tapster, S.; Roberts, N.M.W.; Petterson, M.G.; Saunders, A.D.; Naden, J. From continent to intra-oceanic arc: Zircon xenocrysts record the crustal evolution of the Solomon island arc. *Geology* **2014**, *42*, 1087–1090. [CrossRef]